



Capillary flow of water in tubes partially prefilled with oil

Claudiu Patrascu *[†] and Ioana Rasuceanu [†]*Hydraulics Department, Politehnica University of Bucharest, RO-060042, Romania*

(Received 14 June 2022; accepted 25 October 2022; published 10 November 2022)

The paper is concerned with the capillary flow of water in tubes that are partially prefilled with sunflower oil. We study the system's dynamics as a function of the oil column's length in horizontal and vertical alignments. The study shows that, in a horizontal flow, a spontaneous process of water-droplet formation occurs at the level of the water-oil interface. We investigate this process as a function of the prefilling liquid's volume and describe how to manipulate the location of the breakup event by simply increasing the oil content that prefills the capillary tube. After droplet breakup, experimental observations on capillary intake reveal that for short length scales the liquid-liquid system moves with a constant velocity. We also show how theoretical models can be adapted to predict the position of the water-oil meniscus in time.

DOI: [10.1103/PhysRevFluids.7.114001](https://doi.org/10.1103/PhysRevFluids.7.114001)

I. INTRODUCTION

Capillary flows become dominant liquid transport phenomena when the proper length scale of the system is smaller than the capillary length [1]. At length scales below this threshold, if a capillary tube touches the liquid's free surface, the liquid will spontaneously flow into the tube. These spontaneous liquid flows require no energy input, the system naturally evolving towards a state of total minimum energy. This fact offers an attractive option for the design of autonomous capillary pumping structures, medical diagnostic devices, surface cleaning processes, enhanced oil recovery procedures, and capillarity-driven artificial trees [2–7].

Even at length scales smaller than the capillary length, gravity can alter the dynamics of the liquid invasion. The capillary rise and its gravity-free equivalent, the capillary flow in a horizontal tube, remain central to many academic and applied studies. Although a large number of papers consider a single liquid phase flowing into an empty capillary tube, the problem has also been studied in the context of a liquid phase displacing another immiscible liquid. These studies include the problem of water replacing kerosene in capillary tubes [8], the motion of a water-cyclohexane interface [9], silicone oil-glycerin interfaces [10], silicon oil replacing paraffin oil [11], accompanied by various theoretical models [12–15]. Other closely related studies have tackled the motion of a slug inside a capillary tube driven by a gradient of surfactant concentration [16] and the extraction of a liquid when the slug is placed at the end of the tube [17]. A variety of distinct viscous regimes were reported in the case of a capillary tube completely prefilled with another immiscible viscous fluid [18,19]. In contrast with the capillary flow of one liquid displacing a gaseous phase, liquid-liquid capillary flows remain largely unexplored. The problem is intimately related to practical applications such as surface coating using passive strategies via self-propelled liquid slugs [20,21]. By choosing one liquid phase to be more viscous than the other one could tailor the system's motion to fit various restrictive experimental demands.

*Corresponding author: claudiu.patrascu@upb.ro

[†]These authors contributed equally to this work.

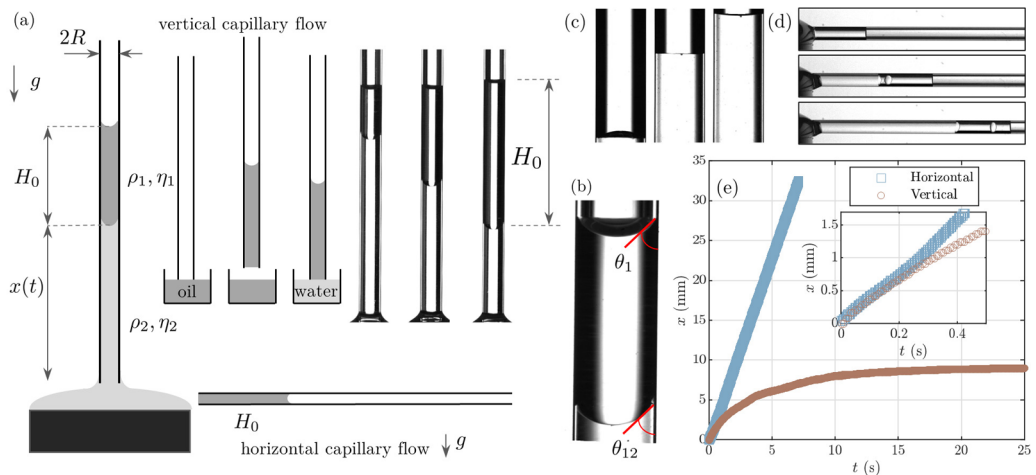


FIG. 1. (a) The schematic illustration of the experimental setup, the prefilling procedure, and a series of images that show the equilibrium height as a function of the prefilling liquid (from left to right H_0 is 3.04, 5.92, 8.84 mm, respectively). The schematic illustration depicts both vertical and horizontal experiments. (b) Image showing the equilibrium contact angles of the oil-air and oil-water interfaces in vertical experiments. (c) Series of images that reveal a change in curvature of the oil-water meniscus as the second liquid (water) invades the capillary (from left to right: concave, flat, and convex). (d) Series of images showing a typical horizontal capillary flow when $H_0 = 5.92$ mm. (e) The position of the oil-air interface as a function of time. Comparison between horizontal and vertical capillary flow when $H_0 = 3.8$ mm. The inset graph shows detail for short times, similar values indicating a capillarity-driven flow.

In this paper, we investigate the capillary flow of water in a tube that was partially prefilled with sunflower oil. We study the system's dynamics as a function of the oil column's length in horizontal and vertical alignments. New phenomena are also reported, such as the curvature change of the oil-water interface during capillary rise and droplet formation in horizontal flows. We also show how theoretical models can be adapted to understand and predict the behavior of the liquid-liquid ensemble. The paper is divided into three main parts, one section showing all experimental details, the other two containing the results obtained in vertical and horizontal alignments of the capillary tube.

II. EXPERIMENTS AND METHODS

A schematic representation of the experimental setup is shown in Fig. 1(a). We used a system of two immiscible liquids, sunflower-seed oil of density $\rho_1 = 920$ kg/m³, viscosity $\eta_1 = 55$ mPa s, surface tension $\gamma_1 = 24$ mN/m, and deionized water of density $\rho_2 = 998$ kg/m³, viscosity $\eta_2 = 1$ mPa s and surface tension $\gamma_2 = 72$ mN/m. The interfacial tension between the two liquids was measured using a pendant method and was found to be $\gamma_{12} = 22$ mN/m. The accuracy of this method is within ± 2 mN/m. We used capillary tubes made of soda-lime glass with an inner diameter of $2R = 0.95$ mm and a length of 5 cm. The capillary tube was first partially prefilled with the more viscous liquid, sunflower oil. Since one of the main control parameters is the oil column's length, H_0 , this action requires an adjustment of the contact time between the capillary tube and the oil bath. When the tube is put in contact with the liquid, the latter starts flowing into the tube. We used a mechanical setup with a micrometer graduation drive mechanism to detach the capillary tube from the liquid bath when it reached the desired position. We emphasize that the prefilling process was done vertically or horizontally, in tandem with the dynamics that were under investigation, i.e., the vertical or the horizontal capillary flow of the liquid-liquid system.

After the prefilling process, the capillary tube was put in contact with water. At this point, a high-speed camera was used, working at more than 500 fps, to record the advance of the liquid-liquid ensemble. Typical examples of such flows are given in Figs. 1(a) and 1(d). The resulting images are then processed with an in-house Matlab routine to identify the position of the oil-air interface. Imperfections in the capillary tube's wall can cause slight deviations in data when repeating the experiment. Several trials were performed to ensure data reproducibility. A typical example is given in Appendix A.

In vertical alignments, the advance of the liquid-liquid system was recorded until it reaches the equilibrium height. The equilibrium contact angles were measured using a built-in routine via the ImageJ software and were found to be $\theta_1 = 46.67 \pm 2.05^\circ$ and $\theta_{12} = 37.70 \pm 3.78^\circ$, oil-air and oil-water meniscus, respectively. A detail is shown in Fig. 1(b).

In horizontal flows, the position of the advancing column was recorded until the oil-air interface reaches the end of the capillary tube. To ensure that the dynamics are solely driven by the wetting properties of the capillary tube, and not influenced by the local curvature of the liquid bath or hydrostatic pressures, that might alter the subsequent dynamics, we compared horizontal and vertical flows for the same volume of the prefilling liquid. Figure 1(e) shows the position of the oil-water interface as a function of time and highlights that gravitational forces bring a significant change to the global dynamics of the system. In contrast, the inset graph shows that the two are very similar for short times (<30 ms), indicating a flow driven solely by capillarity.

III. RESULTS

A. Capillary invasion in vertical tubes

When a capillary tube is aligned vertically and then placed in contact with a liquid bath, the liquid will invade the tube until an equilibrium height is reached. At this point gravitational forces balance capillary forces. The same phenomenon was observed for a capillary tube partially prefilled with sunflower oil. By adjusting the contact time with a liquid bath of oil, the intake of liquid can be controlled. Therefore, different contact times imply different penetration heights H_0 [see Fig. 1(a)]. After the prefilling process, the capillary was brought in contact with a liquid bath of water. The invasion of liquid continues as water displaces the oil phase until the equilibrium height is reached. Soon after the moment of contact, the water-oil interface starts to advance into the capillary tube. The rise velocity of the liquid-liquid system is largely dictated by the more viscous liquid, i.e., the prefilling liquid. The rise velocity of the system decreases because the intake of liquid increases the liquid column's mass.

A peculiar change in the curvature of the water-oil interface was observed. The interface starts with a concave shape immediately after contact. As water invades the capillary, the interface changes from a concave to a convex shape and remains in this form until the equilibrium height is reached. A series of images that show this change in curvature is given in Fig. 1(c). This radical change in curvature is due to the large velocity of the contact line in the first stages of liquid intake. As the liquid invades the capillary tube, weight forces slow down the advance of the contact line eventually bringing the system to rest at the equilibrium height.

We attribute this change in curvature to weight forces that grow in proportion with the intake of water. In the following subsection, we show that the change in curvature is absent for capillary flows in horizontal alignments.

The equilibrium height of the liquid-liquid system can be predicted starting with a general model of capillary rise, which has been adapted for a liquid-liquid system [14]. Considering the balance between capillary forces (as driving forces), the prefilling liquid's weight, the displacing liquid's weight, and viscous forces, we can write:

$$(m_1 + m_2)(\ddot{x} + g) = 2\pi R(\gamma_{ef} - H_0\tau_1 - x\tau_2) - \pi R^2\rho_2\dot{x}^2, \quad (1)$$

where $x = x(t)$ is the position of the water-oil interface, R is the radius of the capillary tube, $m_1 = \pi R^2 H_0 \rho_1$ is the mass of the oil column, $m_2 = \pi R^2 x \rho_2$ is the mass of the water column, $\gamma_{ef} =$

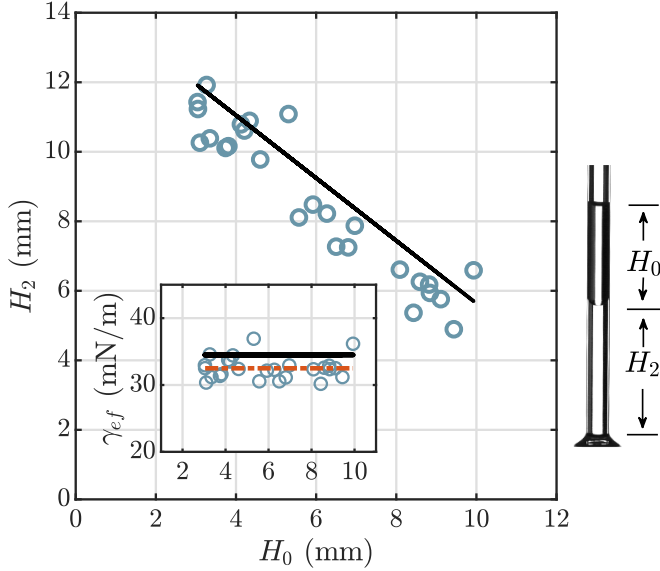


FIG. 2. Equilibrium height, H_2 , reached by the invading liquid and the value of the effective tension (inset graph) as functions of the oil column's length, H_0 . The solid line represents the prediction of Eq. (2) using the measured effective tension, $\gamma_{ef} \approx 34.14$ mN/m. The broken line represents the fit of Eq. (2) having γ_{ef} as the fitting parameter ($\gamma_{ef} \approx 32.5$ mN/m with a coefficient of correlation $R^2 \approx 0.89$).

$\gamma_1 \cos \theta_1 + \gamma_{12} \cos \theta_{12}$ is the effective tension given by the oil-air and the water-oil interfaces (θ_1 and θ_{12} denoting dynamic contact angles), $\tau_{1,2} = 4\eta_{1,2}\dot{x}/R$ are the viscous stresses imparted by the oil (lower index 1) and water columns, respectively. The details of the derivation of Eq. (1) can be found in Appendix B.

The equilibrium height can be obtained under the condition of a static system, $\dot{x} = 0$, therefore

$$\gamma_{ef} - \frac{gR}{2}(\rho_1 H_0 + \rho_2 H_2) = 0 \rightarrow H_2 = \frac{2\gamma_{ef}}{gR\rho_2} - \frac{\rho_1}{\rho_2}H_0, \quad (2)$$

where x has been replaced with H_2 at equilibrium, the water column's length. The equation shows that for a given density ratio, the oil column's length decreases the height at which water should rise. Figure 2 shows a comparison with experimental data for different values of H_0 . For larger columns of the prefilling liquid, the displacing liquid reaches smaller heights. A linear decrease with H_0 of the water column's height H_2 is observed, as predicted by Eq. (2). The predicted values slightly overestimate the height at which water should rise. A fit of the experimental data shows a smaller effective tension, 32.5 mN/m as opposed to the measured value of 34.14 mN/m, which can account for the overestimation, leaving the linear dependence in accordance with Eq. (2). Also, the difference between the measured value and the fitting value is within the margin of error given by the measuring procedure of the surface/interfacial tension.

The position of the water-oil interface as a function of time can be predicted via Eq. (1). The position of the interface varies with time as water displaces the oil phase. Four typical examples are being given in Fig. 3 for various volumes of the prefilling liquid. Given that the capillary tube is prefilled with a liquid that is much more viscous than the displacing liquid, the model given by Eq. (1) can be simplified. First, the timescale t_c of establishing Poiseuille flow (required for boundary effects to diffuse across the tube) can be approximated via the entrance length $L_s/R \approx 0.24\rho\dot{x}R/\eta$. One finds $t_c = L/\dot{x} \approx 0.24\rho R^2/\eta$, which gives: $t_p^w \approx 45$ ms for water and $t_p^o \approx 0.75$ ms for oil. The comparison between the time required for boundary effects to diffuse across the tube and the total transit time, which is three orders of magnitude larger, enables us to neglect the contribution

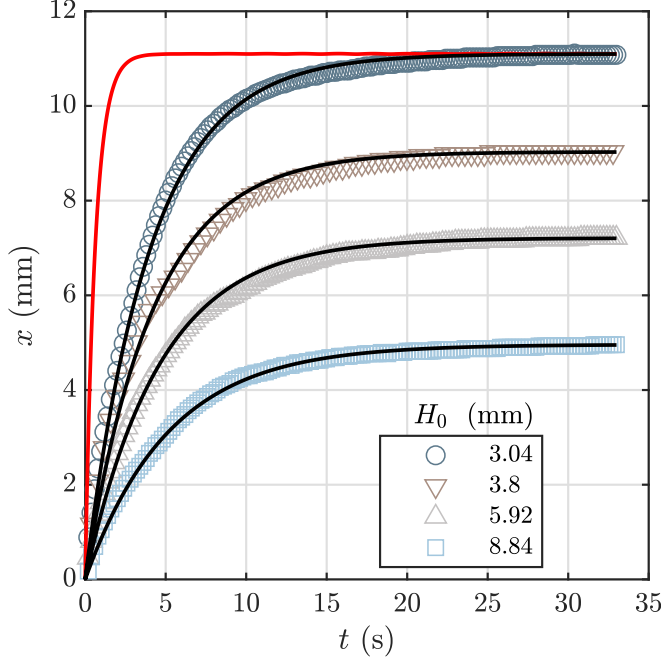


FIG. 3. Measurements of the position of the water-oil interface, in a vertical tube, as a function of time for various volumes of the prefilling liquid and their equivalent fit (continuous line) using the analytical solution of Eq. (6). The average value of the friction coefficient is $\chi = 73 \pm 3$. The red continuous line is the theoretical prediction for $H_0 = 3.04$ mm and $\chi = 0$.

of the inertial terms. We also choose to neglect the the last term of the right-hand side of Eq. (1), because typical rise velocities are in the range of [1,10] mm/s, giving a much smaller contribution when compared to the dominant viscous term, $\rho_2 \dot{x}^2 / (4\eta_1 \dot{x} / R) = \rho_2 \dot{x} R / (4\eta_1) < 0.016$. The model reduces to

$$\dot{x} = \frac{R}{4} \frac{\gamma_{\text{ef}} - \frac{gR}{2}(\rho_1 H_0 + \rho_2 x)}{(\eta_1 H_0 + \eta_2 x)}. \quad (3)$$

The viscous contribution of the invading liquid becomes important when $\eta_1 H_0 \sim \eta_2 x$. Since the viscous forces imparted by the prefilling liquid are 55 times larger, the travel distance at which the viscous contribution of the invading liquid would become of the same order of magnitude is given by $\tau_1 2\pi R H_0 \sim \tau_2 2\pi R X \rightarrow X = 55 H_0$, essentially 55 times larger than the pre-existing column of oil. In our experiments, the smallest column of oil is $H_0 = 2.4$ mm, which gives $X \approx 132$ mm, a distance much larger than the capillary tube that was used (≈ 50 mm). Therefore, we can safely neglect the viscous contribution of the invading liquid. The model simplifies to

$$\dot{x} = \frac{R}{4\eta_1 H_0} \left[\gamma_{\text{ef}} - \frac{gR}{2}(\rho_1 H_0 + \rho_2 x) \right]. \quad (4)$$

The limitations in using the model as a predictive tool are given by the velocity-dependent contact angles. In general, the velocity-dependent dynamic contact angle can be estimated by introducing a friction coefficient [22,23] χ , with which one can write the dynamic contact angle as a function of the static contact angle (reached at equilibrium height) and the velocity of the advancing column, $\gamma \cos \theta_D = \gamma \cos \theta_S - \chi \eta \dot{x}$. For a liquid-liquid system, two velocity-dependent contact angles introduce two friction coefficients. For purely practical purposes, where only predictive power over

the system is wanted, we choose to combine the two friction coefficients into one. An equivalent friction coefficient χ was used for both contact lines (oil-air-glass tube and water-oil-glass tube), having in mind that the prefilling liquid's viscosity is 55 times larger than the invading one's and also assuming that a thin layer of oil lubricates the glass capillary tube. The friction force given by this assumption is $F_r = 2 \times 2\pi R\chi\eta_1\dot{x}$. Under the same assumptions as above, introducing the friction force, neglecting inertia and the viscous contribution of the invading liquid, Eq. (2) can now be written as

$$(m_1 + m_2)g = 2\pi R\gamma_{\text{ef}} - 8\pi\eta_1 H_0\dot{x} - 4\pi R\chi\eta_1\dot{x}, \quad (5)$$

which gives

$$\dot{x} = \frac{R}{4} \frac{[\gamma_{\text{ef}} - \frac{gR}{2}(\rho_1 H_0 + \rho_2 x)]}{\eta_1(H_0 + \frac{R}{2}\chi)}, \quad (6)$$

where γ_{ef} is now calculated with the static contact angles of both interfaces at equilibrium. The analytical solution of the above equation (see Appendix C) was used to fit the experimental data of Fig. 3.

The experimental data in Fig. 3 shows that as H_0 gets larger (more prefilling liquid occupies the capillary), after the capillary tube has touched the water bath, water will invade the capillary and displace the oil column for shorter distances. More prefilling liquid implies larger viscous forces that grow proportional with H_0 . The system's rise velocity will also decrease with H_0 due to an increase in viscous forces.

For a prefilling column of oil equal to $H_0 = 3.04$ mm, we also compare the experimental data with the predictions of Eq. (6) when $\chi = 0$ (red line). As expected, the model overestimates the position of the water-oil interface when no contact angle variation is considered. Introducing the velocity-dependent contact angle via the friction coefficient χ , and using it as a fitting parameter (continuous black line in Fig. 3), provides a good approximation of the water-oil interface's position concerning both time and H_0 . The system's dynamics are described by a friction coefficient $\chi = 73 \pm 3$, an order of magnitude that is similar to those reported in past studies [22,23].

B. Capillary invasion in horizontal tubes

Water invasion due to capillary forces into horizontal tubes that are partially prefilled with oil differs quite substantially compared to the vertical case. In horizontal flows, gravity does not alter the system's dynamics, which interestingly enriches the capillary flow. In this respect, the water-oil interface will form a droplet as the displacing liquid advances, a phenomenon that was not observed in vertical alignments and has not been reported so far in the context of a continuous capillary displacement of another immiscible liquid. A similar phenomenon has been reported for self-propelling liquid slugs [21].

We partially prefill a horizontal capillary tube by putting it in contact with an oil bath. The oil column's length was set by adjusting the contact time. When the prefilled capillary tube touches the liquid bath of water, the liquid-liquid system starts to flow [see Fig. 1(d)]. For short times, the capillary invasion of water shows similarities with the one seen in vertical alignments [see inset graph of Fig. 1(e)]. In a vertically aligned capillary tube, the water-oil interface starts with a concave shape which then progressively changes curvature and turns convex as the displacing liquid advances. In a horizontal flow, the water-oil interface starts, and remains, concave [see Fig. 4(a)], the absence of gravitational forces implying a higher velocity for the liquid-liquid system, which in turn leads to the observed droplet breakup.

Another key difference is the formation of a water droplet during the capillary invasion of water into the partially prefilled tube. Figure 4 shows this process in detail. The pressure gradient that drives the flow from the liquid bath is largely attributed to the negative pressure that settles at the curved oil-air interface. This pressure gradient is large enough to initiate a flow that ultimately causes the water-oil interface to break and form a droplet. After this spontaneous water droplet

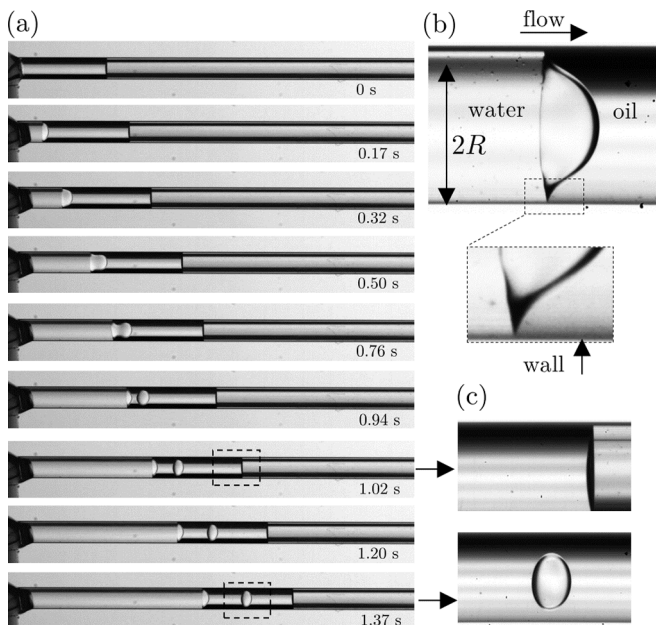


FIG. 4. (a) Series of images showing the invasion of water into a horizontal capillary tube partially prefilled with oil ($H_0 \approx 5$ mm) emphasizing droplet formation. (b) The post-breakup shape of the advancing water-oil interface. The detail shows that the interface changes curvature near the wall via an inflection point. (c) Images showing the oil-air interface and the droplet after the breakup process.

formation, the water-oil interface retains its curvature throughout the displacement process, as shown in Fig. 4(b). As the prefilling column of oil increases in length, the droplet forms at greater distances from the point of liquid intake. Since gravitational forces do not contribute in a horizontal flow by slowing down the advance velocity, the liquid will more rapidly invade the capillary. Given the fact that a thin layer of oil is left behind, the advance of water into the capillary creates the conditions for droplet generation. The lubricant film becomes unstable and the interface naturally evolves towards a state of minimal surface energy by forming a droplet. The process of droplet formation is similar to the formation of a lobe of liquid as observed for a bislug, composed of two wetting liquids, that spontaneously moves in a capillary tube [21].

After droplet break-up, experimental observations on capillary intake show a quasilinear behavior with time for various prefilling columns of oil. The position of the water-oil interface as a function of time can be seen in Fig. 5. As H_0 increases, the velocity of the system decreases. Larger volumes of the prefilling liquid imply larger viscous forces which inevitably lead to smaller displacement velocities. The formation and break-up of the water droplet slow down the capillary intake of water. A typical example can be found in Appendix D. After the water droplet is completely formed the velocity of the system slightly increases and remains approximately constant until it reaches the limit of our experimental setup (given by the length of the capillary tube). To better understand this observed linear variation with time, we turn to the model given by Eq. (3). In the absence of gravitational forces, for a horizontal capillary tube, the model becomes

$$\dot{x} = \frac{R}{4} \frac{\gamma_{ef}}{(\eta_1 H_0 + \eta_2 x)}. \quad (7)$$

If $H_0 = 0$ (no prefilling liquid), then the model reduces to Washburn's law for capillary intake. The differential equation can then be easily solved. Figure 6 shows typical predictions for the position

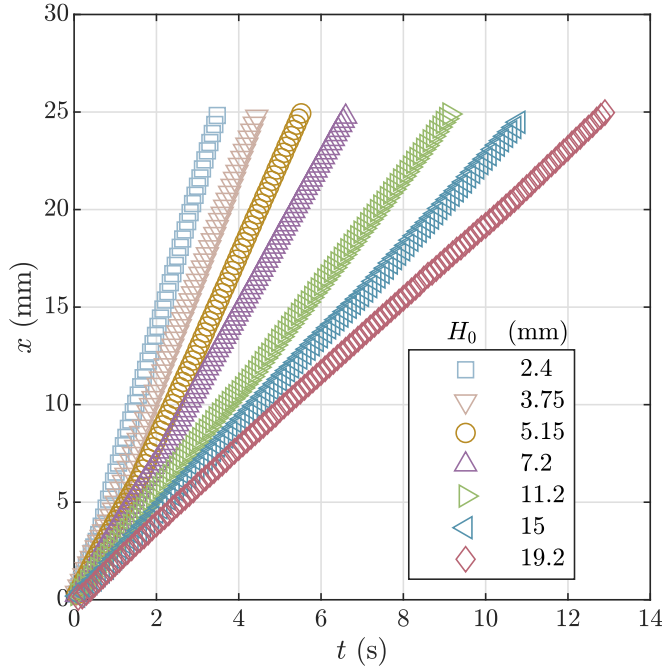


FIG. 5. Measurements of the position of the water-oil interface as a function of time. Horizontal capillary motion in a tube ($R = 0.475$ mm) with various volumes of the prefilling liquid (oil). The invading liquid is water. A quasilinear regime is observed for short travel distances when the prefilling liquid is 55 times more viscous than the second, invading, immiscible liquid.

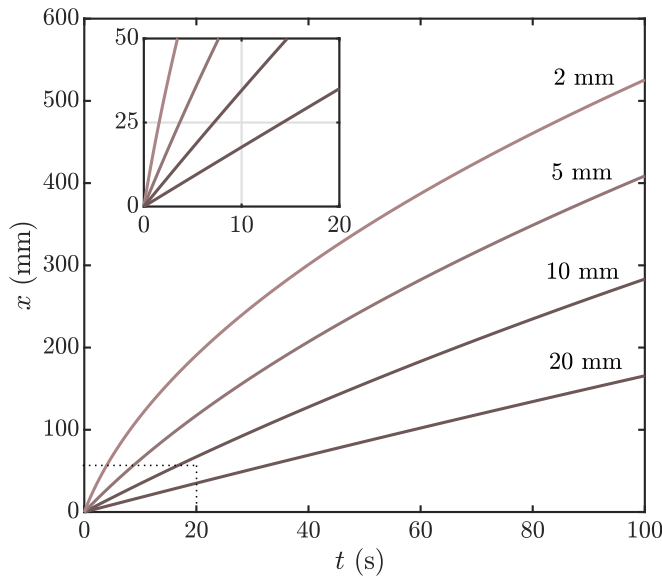


FIG. 6. Changes brought by increasing the volume of the prefilling liquid (i.e., H_0) to the prediction of Eq. (7) in terms of the position of the oil-air interface in a horizontal capillary tube. The inset graph shows a detail of the predictions for short travel distances. (The relevant parameters are $\eta_1 = 55$ mPa s, $\eta_2 = 1$ mPa s, $\gamma_{ef} = 16.5$ mN/m, $R_0 = 0.475$ mm.)

of the water-oil interface as a function of time. For a given observation time, as H_0 increases, the prediction resembles more closely with a linear regime. This can also be seen in the inset graph for smaller observation length scales. The same quasilinear regime is found as a result of the prefilling liquid.

We wish to approximate the velocities of the liquid-liquid systems that are given in Fig. 5, as a function of H_0 . Since the viscosity of the prefilling liquid is 55 times larger, the viscous effects brought by the displacing liquid become important at length scales given by $\eta_1 X \sim \eta_2 H_0 \rightarrow X \sim 55 H_0$. For a 50 mm capillary tube ($50 \text{ mm} \ll 55 H_0$) viscous dissipation is mainly given by the prefilling liquid. Discarding the viscous effects of the displacing liquid, Eq. (7) becomes

$$\dot{x} \approx \frac{R\gamma_{\text{ef}}}{4\eta_1 H_0}, \quad (8)$$

where $\gamma_{\text{ef}} = \gamma_1 \cos \theta_1 + \gamma_{12} \cos \theta_{12}$. After the formation of the water droplet, the water-oil interface settles into a shape that changes curvature near the wall via an inflection point. A typical shape of the water-oil interface is shown in Fig. 4(c). This observational fact allows us to assume $\cos \theta_{12} \approx 0$ ($\theta_{12} \approx 90^\circ$) which implies that the effective driving tension is mainly given by the oil-air interface, $\gamma_{\text{ef}} \approx \gamma_1 \cos \theta_1$.

To tackle the problem of the velocity-dependent contact angle, we consider the classical approach as given by De Gennes [24]. The motion of the liquid-liquid system in the capillary tube is similar to the motion of a self-propelled liquid bi-slug [21], the model being in fair agreement with experimental data. For contact angles between $[0^\circ, 120^\circ]$ it is known that the contact angle scales as $(\eta_1 \dot{x} / \gamma_1)^{1/3}$. For small contact angles, by balancing the viscous force with the noncompensated capillary force in the vicinity of the contact line, one obtains

$$\theta_1 = (6\Gamma \eta_1 \dot{x} / \gamma_1)^{1/3}, \quad (9)$$

where $\Gamma \approx 15$ is a prefactor related to physical cutoffs. The contact angle of the advancing oil-air interface is approximately 21.8° which permits us to use $\cos \theta_1 \approx 1 - \theta_1^2/2$ as an approximation for the cosine function. Using the above relation in tandem with Eqs. (8) and (9), we obtain

$$\dot{x} - \frac{V_0}{2} \left[2 - \left(\frac{6\Gamma \eta_1 \dot{x}}{\gamma_1} \right)^{2/3} \right] = 0, \quad (10)$$

where $V_0 = R\gamma_1/(4\eta_1 H_0)$ and γ_1 is the surface tension of the prefilling liquid, in our case sunflower oil.

Next, we take the linear fit of the experimental data (see, for example, Fig. 5) and plot the resulting velocities as a function of H_0 . Figure 7(a) illustrates the comparison with the predictions of Eq. (10). The model proves to be a good approximation of the observed data. The model captures well the decrease in velocity when the capillary tube contains more oil (larger values for H_0). The data are also compared with the case when oil completely wets the capillary tube, $\theta_1 = 0$, $V_0 = R\gamma_1/(4\eta_1 H_0)$; solid line in Fig. 7. When the capillary tube contains less oil (small H_0), the discrepancy between the latter prediction and experimental data is large. If, in turn, the capillary tube contains more oil, then both experimental data and prediction approach the limit given by the case when the liquid completely wets the capillary. The two predictions (solid and broken line of Fig. 7) get closer and closer as H_0 increases. This implies that, for a large volume of liquid prefilling the capillary tube, the effect introduced by the dynamic nature of the contact angle is negligible.

Experiments show that the position along the capillary tube at which a water droplet is formed (H_b) increases with the oil column's length, H_0 , as depicted in Fig. 7(b). This observation allows one to manipulate the location of the breakup event by simply increasing the oil content that prefills the capillary tube.

The model given by Eq. (10) can also be used to approximate the speed with which the system generates a droplet. This was done by measuring the distance along the capillary tube at which

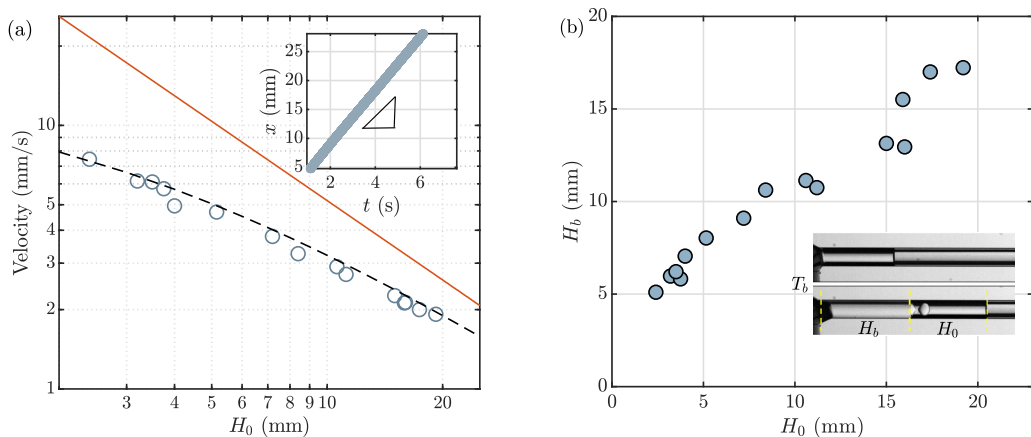


FIG. 7. (a) The velocity of the liquid-liquid ensemble, after the formation of the droplet, as a function of the oil column's length, H_0 . The circles depict the linear fit of experimental data (see inset graph), the broken line shows the prediction of Eq. (10), and the solid line represents $V_0 = R\gamma_1/(4\eta_1 H_0)$. (b) The position along the capillary tube at which a water droplet is formed, H_b , as a function of the oil column's length, H_0 . The inset image depicts both H_b and H_0 at the droplet formation event.

the droplet is formed, H_b , and the corresponding time, T_b . The ratio H_b/T_b gives a measure in this respect. We measured H_b and T_b for several values of H_0 . It can be observed that the droplet generation speed is well approximated by the model, especially for large values of H_0 . We also emphasize small differences when compared to the velocity with which the system moves after droplet break-up [illustrated in Fig. 7(a)]. This can be understood if we consider that the extra-dissipating forces induced by the formation and break-up process are smaller than those given by the prefilling oil column. This can also be seen when we look at the position of the water-oil interface with respect to time. The break-up event does change the dynamics of the system but only by a small amount when H_0 is large (see Figs. 5 and 10).

IV. CONCLUSIONS

When a capillary tube touches the free surface of a liquid, a spontaneous flow will drive the liquid into the capillary. This situation also applies for a capillary tube that has been partially prefilled with a more viscous liquid that subsequently touches a less viscous immiscible liquid. We study this situation when water displaces sunflower oil in horizontal and vertical alignments of the capillary tube.

In the case of vertical tubes, we find a similar manifestation with the classical case described by the capillary rise of one liquid phase displacing air. A similar form of Jurin's law describes the equilibrium height reached by the liquid-liquid system when varying the oil column's length. Experimental observations show that, as the displacing liquid invades the capillary tube, the water-oil interface, which starts off as a concave-shaped meniscus, changes curvature. As the water column grows in weight, the meniscus changes from concave to convex and eventually reaches the equilibrium height. For purely practical purposes that would require knowing the position of the water-oil meniscus as a function of time or as a function of the prefilling liquid's volume, we show that classical models can be adapted to approximate the dynamics of the liquid-liquid system.

Horizontal capillary flows of a water-oil system, when the prefilling liquid is oil, show substantial differences. As the less viscous phase invades the prefilled capillary, it also starts a process of droplet

generation. A water droplet forms at the level of the water-oil meniscus at increasing distances from the intake point as the prefilling liquid occupies larger portions of the capillary tube. For short length scales, the dynamics can be well approximated by neglecting the viscous dissipation of the invading liquid. At these length scales, we find the advance velocity of the liquid-liquid system to be approximately constant. Experimental observations show that the driving, effective tension is mainly given by the oil-air meniscus and its time-dependent behavior. We also show how models can be adapted to predict the velocity of the system when droplet generation occurs naturally in partially prefilled capillary tubes.

ACKNOWLEDGMENTS

The experimental investigations were possible due to European Regional Development Fund through Competitiveness Operational Program 2014–2020, Priority axis 1, Project No. P-36-611, MySMIS code 107066, Innovative Technologies for Materials Quality Assurance in Health, Energy and Environmental–Center for Innovative Manufacturing Solutions of Smart Biomaterials and Biomedical Surfaces INOVABIOMED. The authors acknowledge the support of CHIST-ERA 19 XAI 009 MUCCA project, by the founding of EC and The Romania Executive Agency for Higher Education, Research, Development and Innovation Funding–UEFISCDI, Grant COFUND-CHIST-ERA MUCCA No. 206/2019. The experiments were carried out in part in the Reorom Laboratory–UPB, for which the authors thank professor Corneliu Balan.

APPENDIX A: DATA REPRODUCIBILITY

Figure 8 shows the position of the water-oil interface as a function of time for both horizontal and vertical capillary flows. Similar oil column lengths give approximately the same time-dependent outcome.

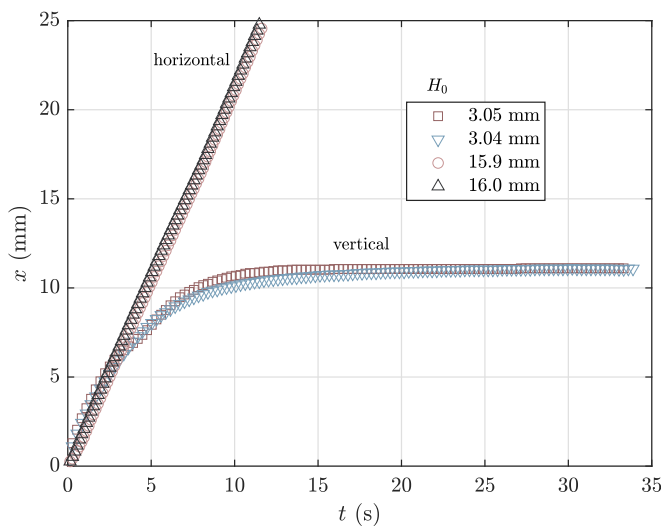


FIG. 8. Horizontal vs vertical capillary flows for similar column lengths H_0 of the prefilling liquid (sunflower oil).

APPENDIX B: DERIVATION OF THE MODEL

Rate of change of momentum dictates

$$\frac{d}{dt}[(m_1 + m_2)\dot{x}] = \sum F_i. \quad (\text{B1})$$

The left-hand side can be written as

$$\frac{d}{dt}[(m_1 + m_2)\dot{x}] = m_1\ddot{x} + \dot{m}_2\dot{x} + m_2\ddot{x} = (m_1 + m_2)\ddot{x} + \pi R^2 \rho_2 \dot{x}^2, \quad (\text{B2})$$

where m_1 is constant and represents the mass of the prefilling liquid.

The tensile force that drives the motion is resisted by weight forces and viscous stresses. The right-hand side now reads

$$\sum F_i = 2\pi R(\gamma_{\text{ef}} - H_0\tau_1 - x\tau_2) - (m_1 + m_2)g. \quad (\text{B3})$$

We obtain

$$(m_1 + m_2)(\ddot{x} + g) = 2\pi R(\gamma_{\text{ef}} - H_0\tau_1 - x\tau_2) - \pi R^2 \rho_2 \dot{x}^2. \quad (\text{B4})$$

APPENDIX C: ANALYTICAL SOLUTION OF THE MODEL

The reduced model for the capillary rise of the displacing liquid is given by

$$\dot{x} = \frac{R}{4} \frac{\gamma_{\text{ef}} - \frac{gR}{2}(\rho_1 H_0 + \rho_2 x)}{\eta_1(H_0 + \frac{R}{2}\chi)}. \quad (\text{C1})$$

Since the addition of the contact line friction coefficient only implies replacing $\eta_1 H_0$ with $\eta_1(H_0 + \chi R/2)$, we describe the case when $\chi = 0$, which is given by

$$\dot{x} = \frac{R\gamma_{\text{ef}}}{4\eta_1 H_0} \left[1 - \frac{\rho_1 g R H_0}{2\gamma_{\text{ef}}} \left(1 + \frac{\rho_2 x}{\rho_1 H_0} \right) \right], \quad (\text{C2})$$

where $x = x(t)$. We propose a dimensionless variant of the above equation for the purpose of making the analytical procedure more traceable. The dimensionless parameters are: $\hat{x} = x/H_0$, $d\hat{x}/d\hat{t} = \dot{x}/V_0$, with $V_0 = R\gamma_{\text{ef}}/(4\eta_1 H_0)$, $\zeta = \rho_2/\rho_1$, and $\text{Bo} = \rho_1 g R H_0/(2\gamma_{\text{ef}})$ as a modified Bond number. The resulting dimensionless equation reads as

$$d\hat{x}/d\hat{t} = 1 - \text{Bo} - \text{Bo} \zeta \hat{x}. \quad (\text{C3})$$

Since in our experiments $\zeta \approx 1.1$, $\text{Bo} \sim \mathcal{O}(10^{-3})$, and $\hat{x} < 10$, $(1 - \text{Bo})$ and the right hand side of the above equation are always positive. Integrating, we obtain

$$\int_0^{\hat{x}} \frac{d\hat{x}}{1 - \text{Bo} - \text{Bo} \zeta \hat{x}} = \int_0^{\hat{t}} d\hat{t} \rightarrow \hat{x} = \frac{1 - \text{Bo}}{\text{Bo} \zeta} (1 - e^{-\text{Bo} \zeta \hat{t}}), \quad (\text{C4})$$

which gives

$$x(t) = \frac{2\gamma_{\text{ef}} - \rho_1 g R H_0}{\rho_2 g R} \left(1 - e^{-\frac{\rho_2 g R^2}{8\eta_1 H_0} t} \right). \quad (\text{C5})$$

Introducing the effective tension at equilibrium via

$$\gamma_{\text{ef}} = \frac{R}{2}(\rho_1 g H_0 + \rho_2 g H_2), \quad (\text{C6})$$

and the contact line friction coefficient by replacing $\eta_1 H_0$ with $\eta_1(H_0 + \chi R/2)$, we obtain

$$x(t) = H_2 \left[1 - \exp \left(-\frac{\rho_2 g R^2}{8\eta_1(H_0 + \frac{R}{2}\chi)} t \right) \right]. \quad (\text{C7})$$

Here, H_2 is the displacing liquid's equilibrium height. The analytical solution is identical with the numerical solution of Eq. (C1) found via Matlab as shown in Fig. 9. The friction coefficient was then considered as a fitting parameter using numerical built-in procedures in Origin.

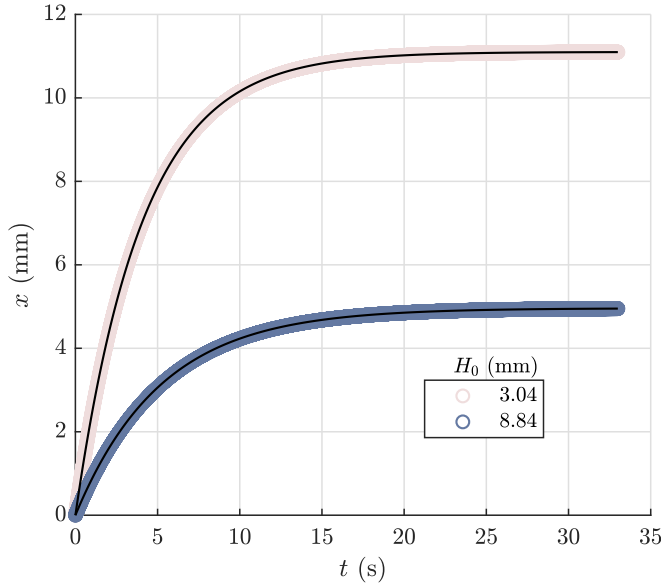


FIG. 9. The analytical solution of Eq. (C1) and its equivalent numerical solution obtained in Matlab. The continuous black line denotes the analytical solution in the form given by Eq. (C7).

APPENDIX D: THE EFFECT OF THE DROPLET FORMATION PROCESS

Figure 10(a) shows the effect of droplet formation and break-up on the dynamics of the liquid-liquid system for two values of the oil column's length, H_0 . Figure 10(b) shows the ratio H_b/T_b as a function of H_0 . Here, H_b/T_b represents the slope of the linear approximation of the position of the system with respect to time to the point of droplet formation. Both H_b and T_b are measured at the breakup event.

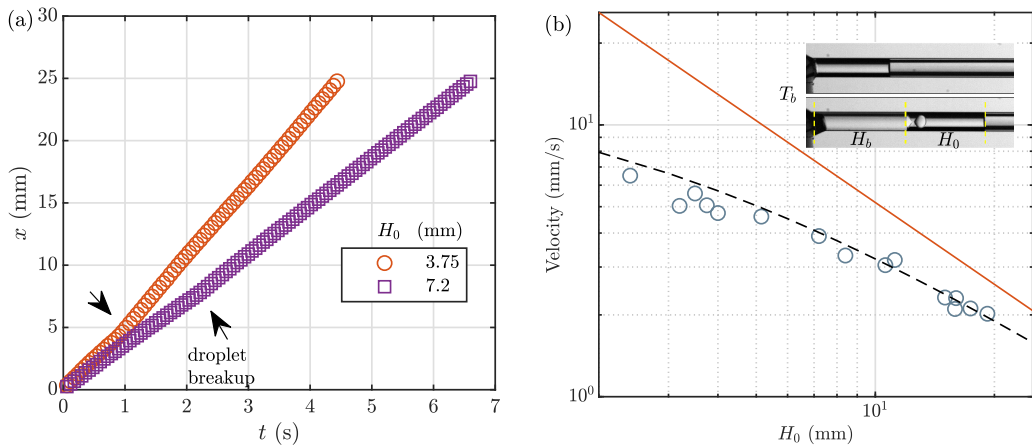


FIG. 10. (a) Depiction of two droplet-breakup events in horizontal, partially prefilled, capillary tubes. (b) Same as in Fig. 7(a) with the difference that here the experimental velocities are computed with H_b/T_b , the ratio between the position at which droplet breakup occurs, H_b , and the corresponding travel time, T_b .

- [1] A. Ponomarenko, D. Quéré, and C. Clanet, A universal law for capillary rise in corners, *J. Fluid Mech.* **666**, 146 (2011).
- [2] M. Zimmermann, H. Schmid, P. Hunziker, and E. Delamarche, Capillary pumps for autonomous capillary systems, *Lab Chip* **7**, 119 (2007).
- [3] W. Guo, J. Hansson, and W. van der Wijngaart, Capillary pumping independent of the liquid surface energy and viscosity, *Microsyst. Nanoeng.* **4**, 1 (2018).
- [4] P. Novo, F. Volpetti, V. Chu, and J. P. Conde, Control of sequential fluid delivery in a fully autonomous capillary microfluidic device, *Lab Chip* **13**, 641 (2013).
- [5] F.-C. Wang and H.-A. Wu, Enhanced oil droplet detachment from solid surfaces in charged nanoparticle suspensions, *Soft Matter* **9**, 7974 (2013).
- [6] B. A. Suleimanov, F. Ismailov, and E. Veliyev, Nanofluid for enhanced oil recovery, *J. Pet. Sci. Eng.* **78**, 431 (2011).
- [7] T. D. Wheeler and A. D. Stroock, The transpiration of water at negative pressures in a synthetic tree, *Nature (London)* **455**, 208 (2008).
- [8] A. Calvo, I. Paterson, R. Chertcoff, M. Rosen, and J. Hulin, Dynamic capillary pressure variations in diphasic flows through glass capillaries, *J. Colloid Interface Sci.* **141**, 384 (1991).
- [9] R. Chertcoff, A. Calvo, I. Paterson, M. Rosen, and J. Hulin, Transient effects in liquid-liquid interface motions through glass capillaries, *J. Colloid Interface Sci.* **154**, 194 (1992).
- [10] M. Fermigier and P. Jenffer, An experimental investigation of the dynamic contact angle in liquid-liquid systems, *J. Colloid Interface Sci.* **146**, 226 (1991).
- [11] P. Van Remoortere and P. Joos, Spontaneous liquid/liquid displacement in a capillary, *J. Colloid Interface Sci.* **160**, 397 (1993).
- [12] T. E. Mumley, C. Radke, and M. C. Williams, Kinetics of liquid/liquid capillary rise: I. Experimental observations, *J. Colloid Interface Sci.* **109**, 398 (1986).
- [13] T. E. Mumley, C. Radke, and M. C. Williams, Kinetics of liquid/liquid capillary rise: II. Development and test of theory, *J. Colloid Interface Sci.* **109**, 413 (1986).
- [14] W. Chan and C. Yang, Surface-tension-driven liquid-liquid displacement in a capillary, *J. Micromech. Microeng.* **15**, 1722 (2005).
- [15] S. Prokopev, A. Vorobev, and T. Lyubimova, Phase-field modeling of an immiscible liquid-liquid displacement in a capillary, *Phys. Rev. E* **99**, 033113 (2019).
- [16] K. Piroird, C. Clanet, and D. Quéré, Detergency in a tube, *Soft Matter* **7**, 7498 (2011).
- [17] K. Piroird, C. Clanet, and D. Quéré, Capillary extraction, *Langmuir* **27**, 9396 (2011).
- [18] P. L. Walls, G. Dequidt, and J. C. Bird, Capillary displacement of viscous liquids, *Langmuir* **32**, 3186 (2016).
- [19] J. André and K. Okumura, Capillary replacement in a tube prefilled with a viscous fluid, *Langmuir* **36**, 10952 (2020).
- [20] J. Bico and D. Quere, Liquid trains in a tube, *Europhys. Lett.* **51**, 546 (2000).
- [21] J. Bico and D. Quéré, Self-propelling slugs, *J. Fluid Mech.* **467**, 101 (2002).
- [22] P. Wu, A. D. Nikolov, and D. T. Wasan, Two-phase displacement dynamics in capillaries-nanofluid reduces the frictional coefficient, *J. Colloid Interface Sci.* **532**, 153 (2018).
- [23] T. Andruk, D. Monaenkova, B. Rubin, W.-K. Lee, and K. G. Kornev, Meniscus formation in a capillary and the role of contact line friction, *Soft Matter* **10**, 609 (2014).
- [24] P.-G. De Gennes, Wetting: Statics and dynamics, *Rev. Mod. Phys.* **57**, 827 (1985).